Poly(methyl methacrylate)−Poly(caprolactone) AB and ABA Block Copolymers by Combined Ring-Opening Polymerization and Atom Transfer Radical Polymerization

Michèle Schappacher, Nicolas Fur, and Sophie M. Guillaume*

Laboratoire de Chimie des Polymères Organiques, CNRS-ENSCPB, Université Bordeaux 1, ENSCPB, 16 Avenue Pey-Berland, 33607 Pessac Cedex, France

Received February 16, 2007; Revised Manuscript Received September 25, 2007

ABSTRACT: Chemical modification of α-hydroxy,ω-isopropylestertelechelic *i*PrO−PCL−OH, **1**, and α,ω-dihydroxytelechelic HO−PCL−OH, **4**, poly(ϵ-caprolactone) (PCL), synthesized from ring-opening polymerization using $La(O^iPr)_3$ or $Sm(BH_4)_3(THF)_3$, allows the synthesis of the corresponding α-bromoester end-functionalized polymers *i*PrO−PCL−Br, **2**, and Br−PCL−Br, **5**, respectively. This direct procedure consists in an esterification of the hydroxy group(s) of **1** and **4** using 2-bromoisobutyryl bromide. These bromopolyesters **2** and **5** have subsequently been used as macroinitiators to synthesize, via atom transfer radical polymerization of methyl methacrylate (MMA), the new set of di- and triblock polyester−polyacrylate copolymers PCL-*b*-PMMA, **3**, and PMMA-*b*-PCL-*b*-PMMA, **6**, respectively. All (co)polymers are well defined as characterized by NMR and size exclusion chromatography analyses. In addition, the thermal properties of copolymers **3** and **6** have been investigated by differential scanning calorimetry. The self-assembly of triblock PMMA-*b*-PCL-*b*-PMMA, **6**, copolymers into nanoparticles has been investigated by dynamic light scattering, atomic force microscopy, and optical microscopy techniques.

Introduction

Block copolymers have received extensive attention from academia and industry because of their remarkable ability to spontaneously assemble into nanoscale polymeric architectures.[1,2] Amphiphilic block copolymers, composed of a hydrophilic block chemically bound to a hydrophobic one, have attracted increasing interest as polymeric micelles in pharmaceutical applications ranging from sustained-release technologies to gene delivery.[3−6] However, such amphiphilic block copolymers, specifically composed of biocompatible polymers, remain nowadays undeveloped.[7] To that end, we are elaborating polyester−polypeptide-based diblock and triblock architectures to design novel drug-delivery systems.[8−10] For this same purpose, we are now extending our research to polyester−polyacrylate copolymers. Indeed, such copolymers are of interest as support for controlled drug delivery.[11−14] As a first approach, we have focused our initial investigations on typical monomers as models, namely, ϵ-caprolactone and methyl methacrylate, prior to considering other hydrophobic polyester associated to hydrophilic acrylate blocks.

Synthetic pathways to gain access to block copolymers follow two general strategies. One traditional approach relies upon the sequential block copolymerization using a two-step route, provided that the first polymerization is a living reaction and given that both monomers can be polymerized via the same chemical process. The second way to prepare block copolymers involves a three-step method. First, one polymer has to be polymerized, then it should be appropriately postfunctionalized before being used as a macroinitiator for the second monomer polymerization. The transformation sequence can take place directly on the active propagation center of the first block or on the chain end(s) of the first isolated polymer. Prefunctionalization of the first monomer prior to its dual polymerization is another option in this last procedure.

For the synthesis of polyester−polyacrylate block copolymers, we have been investigating both strategies starting with poly(ϵ-caprolactone) (PCL) and poly(methyl methacrylate) (PMMA) as models. First, the living characteristic of the polymerization of CL initiated by rare earth alkoxide or borohydride derivatives that we established in the previous studies prompted us to study the block copolymerization with MMA.[15−18] However, such a pathway remained unsuccessful. Similarly, MMA polymerization followed by CL addition, using these same initiators, did not allow us in preparing the desired PCL-*b*-PMMA copolymers.[19]

We next investigated the second three-step strategy involving the synthesis of PCLs, their chemical functionalization, and their subsequent copolymerization with MMA. This particular approach relies on the availability of the valuable monohydroxyl- and especially dihydroxyl-terminated PCLs synthons, which we have developed and have otherwise already chemically functionalized. Indeed, we reported recently on the chemical modification of α-hydroxy,ω-isopropyltelechelic *i*PrO−PCL−OH, **1**, and α,ω-dihydroxytelechelic HO-PCL-OH, **4**, polyesters to amino end-functionalized analogues *i*PrO−PCL−NH_2 and H_2N−PCL−NH_2, respectively.[8] These aminopolyesters were then successfully used as macroinitiators to access the new biomacromolecular diblock and triblock polyester−polypeptide copolymers, PCL-*b*-PBLG (PBLG = poly(γ-benzyl L-glutamate)) and PBLG-*b*-PCL-*b*-PBLG. Herein, we report on the chemical modification of these hydroxyl-functionalized PCLs **1** and **4**, prepared from ring-opening polymerization (ROP) of CL using $La(O^iPr)_3$ or $Sm(BH_4)_3(THF)_3$,[15−17] to the bromo-terminated PCLs and their subsequent use as macroinitiators for the atom transfer radical polymerization (ATRP) of methyl methacrylate to form PCL−PMMA copolymers. Both di- and triblock copolymers have been prepared, with such a set of PMMA/

* To whom correspondence should be addressed. E-mail address: sophie.guillaume@univ-rennes1.fr. Phone: (+33)2 2323 5880. Fax: (+33)2 2323 6939. Present address: Université de Rennes 1, UMR 6226-Catalyse et Organométalliques, Campus de Beaulieu, 35042 Rennes Cedex, France.

10.1021/ma070417q CCC: $37.00
Published on Web 11/07/2007

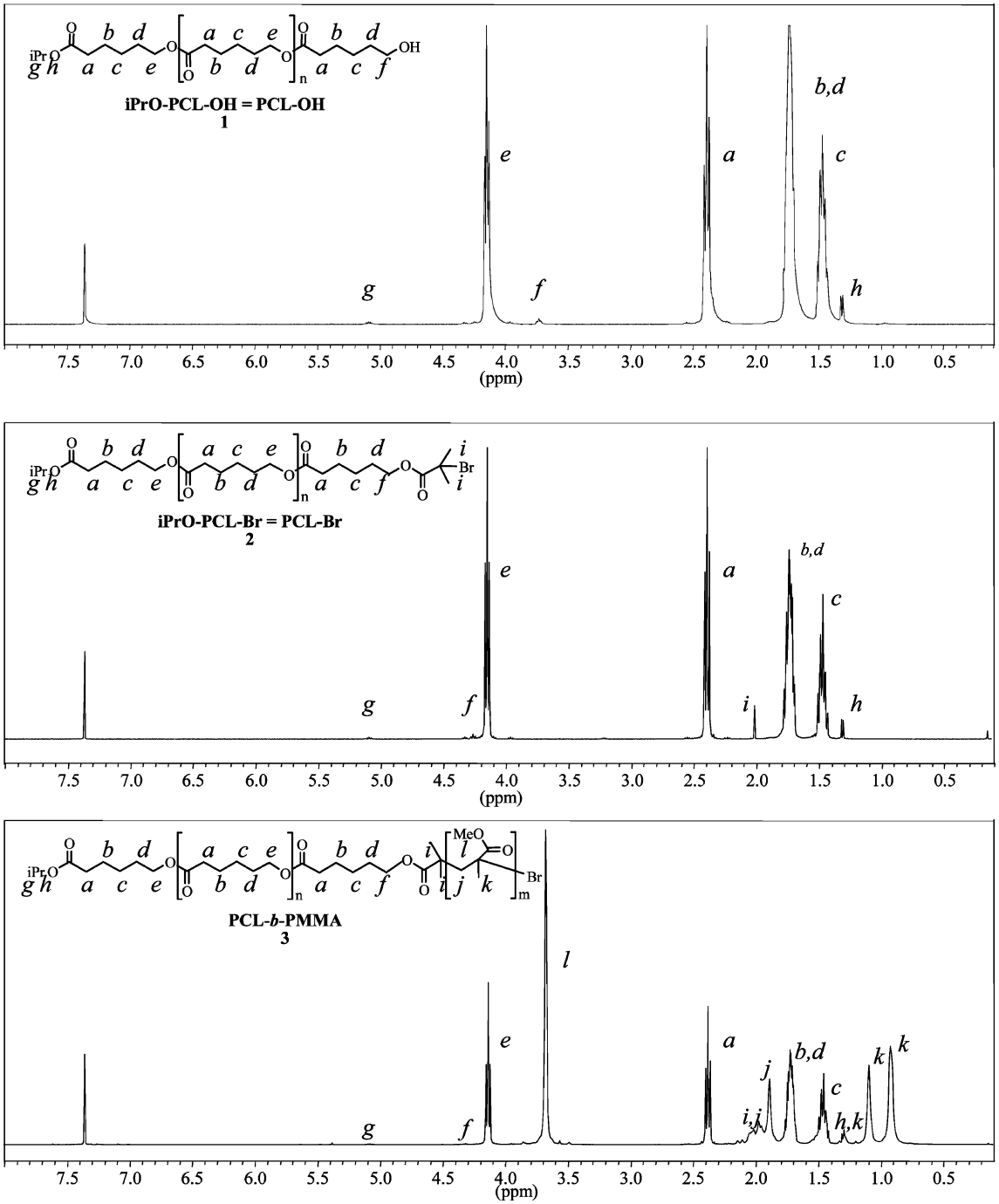

Figure 1. ^{1}H NMR spectra in $CDCl_3$ of PCL_{94}−OH, **1**, PCL_{94}−Br, **2**, and PCL_{94}-*b*-$PMMA_{195}$, **3**.

PCL analogous copolymers being obtained here for the first time. We thoroughly characterized these copolymers by NMR, kinetics, and thermal analyses and also examined the self-assembling behavior of the triblock copolymers.

Experimental Section

Materials. All manipulations were performed under inert atmosphere using standard Schlenk and vacuum line techniques. Solvents were thoroughly dried and deoxygenated by standard methods and distilled before use. $CDCl_3$ was dried over a mixture of 3 and 4 Å molecular sieves. Methyl methacrylate (MMA) was dried and stored over CaH_2. 2-Bromoisobutyril bromide, NEt_3, CuBr, and pentamethyldiethylenetriamine (PMDETA) were used as received. *i*PrOC(O)$(CH_2)_5$O{C(O)$(CH_2)_5$O}$_n$C(O)$(CH_2)_5$OH, iPrO−PCL−OH = PCL-OH, **1**, and HO$(CH_2)_5$C(O){O$(CH_2)_5$C(O)}$_n$O$(CH_2)_6$OH, HO-PCL-OH = PCL-OH_2, **4**, polymer samples were synthesized and characterized according to reported procedures.[15−17]

^{1}H NMR of **1**: δ = 5.10 (quintuplet, 1H, C*H*$(CH_3)_2$); 4.15 (t, $(2n + 2)$H, CH_2O); 3.72 (t, 2H, CH_2OH); 2.39 (t, $(2n + 4)$H, C(O)-CH_2); 1.71 (m, $(4n + 8)$H, CH_2CH_2CH_2); 1.48 (m, $(2n + 4)$H, CH_2CH_2CH_2); 1.31 (d, 6H, CH(CH_3)$_2$) (Figure 1). ^{1}H NMR of **4**: δ = 4.05 (t, $(2n+2)$H, CH_2O); 3.62 (t, 4H, CH_2OH); 2.30 (t, $(2n + 2)$H, C(O)CH_2); 1.64 (m, $(4n + 8)$H, CH_2CH_2CH_2); 1.38 (m, $(2n + 6)$H, CH_2CH_2CH_2) (Figure 2).

Instrumentation and Measurements. ^{1}H (400 MHz) and ^{13}C (100 MHz) NMR spectra were recorded in $CDCl_3$ on a Bruker Avance DPX 400 at 23 °C and were referenced internally using the residual ^{1}H and ^{13}C solvent resonances relative to tetramethylsilane (δ = 0).

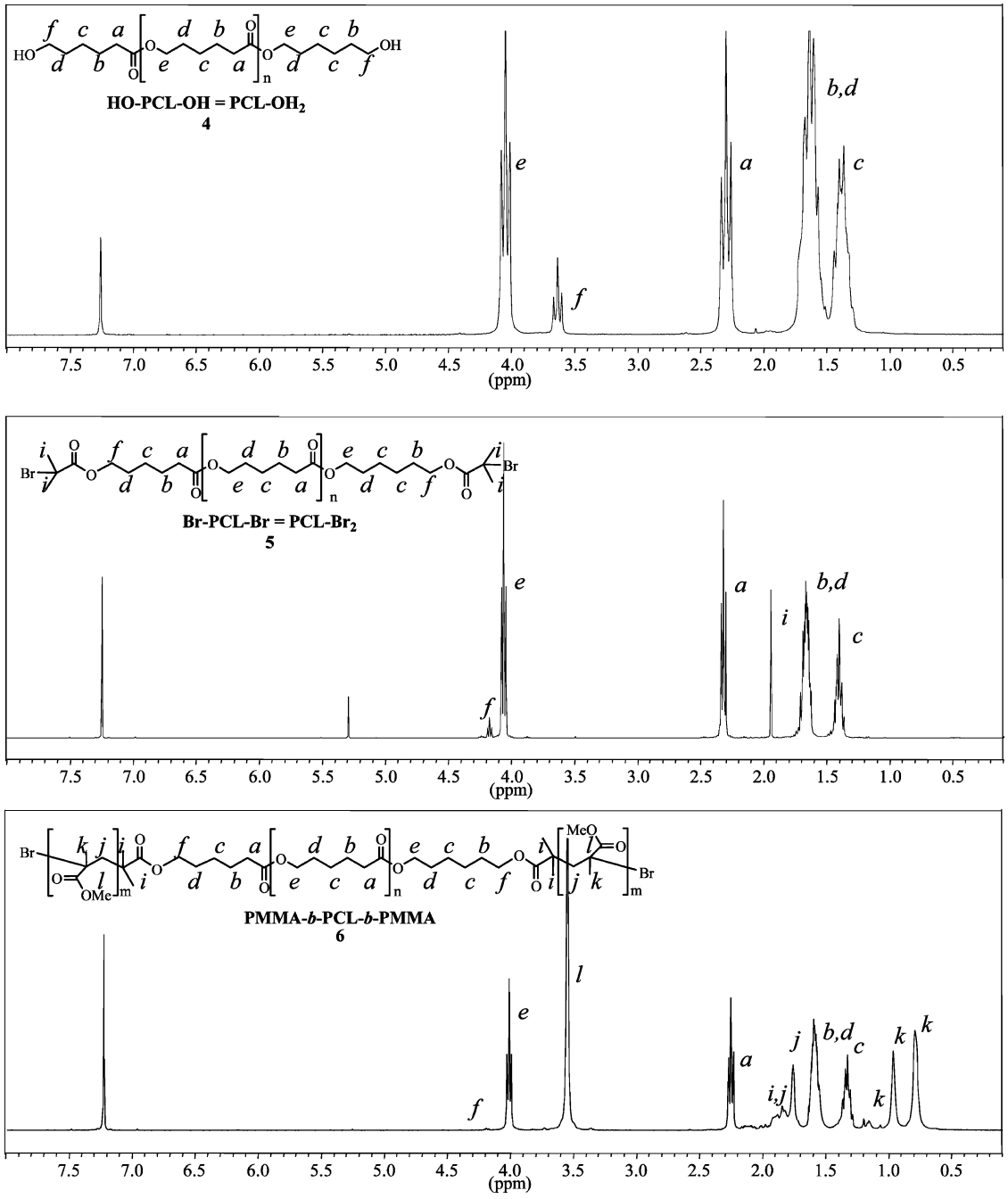

Figure 2. ^{1}H NMR spectra in $CDCl_3$ of $PCL_{32}-OH_2$, **4**, $PCL_{32}-Br_2$, **5**, and $PMMA_{54}$-*b*-PCL_{32}-*b*-$PMMA_{54}$, **6**.

Average molar mass ($\bar{M}_n$) and molar mass distribution ($\bar{M}_w/\bar{M}_n$) values were determined from chromatogram traces recorded on a size exclusion chromatography (SEC) instrument (Varian) in tetrahydrofuran (THF) at 20 °C (flow rate of 1.0 mL min^{-1}) equipped with a refractive index detector and three TSK HXL columns G2000, 3000, and 4000. The polymer samples were dissolved in THF (2 mg mL^{-1}). All elution curves were calibrated with polystyrene standards. $\bar{M}_{n,SEC}$ values of PCLs (PCL−$OH_{1,2}$ and PCl−$Br_{1/2}$) were calculated using the correction coefficient previously reported ($\bar{M}_{n,SEC} = \bar{M}_{n,SECraw\ data} \times 0.56$).[15−18,20] $\bar{M}_{n,SEC}$ values of PMMA block(s) in the copolymers were calculated using the correction coefficient established from PMMA standards ($\bar{M}_{n,SEC} = \bar{M}_{n,SECraw\ data} \times 0.90$). Molar mass values of block copolymers were thus determined from SEC using the corresponding correction coefficient and composition of each block ($\bar{M}_{n,SEC} = \bar{M}_{n,SECraw\ data} \times 0.56 \times comp._{PCL}) + (\bar{M}_{n,SECraw\ data} \times 0.90 \times comp._{PMMA})$).

Monomer conversions were calculated from ^{1}H NMR spectra of the crude polymer samples from the integration (Int.) ratio Int. P(ϵ-CL)/[Int. P(ϵ-CL) + Int. (ϵ-CL)] using the methylene group in the α-position of the carbonyl ($CH_2C(O)$, $\delta = 2.39-2.30$ ppm) for CL and by gravimetry for MMA.

Number average degrees of polymerization $\overline{DP}n$ were determined from ^{1}H NMR analyses; the values resulted from the integration ratio of the main chain (OCH_2, 2*n*H) signal at $\delta = 4.15-4.05$ ppm relative to the end group methylene proton (CH_2OH, 4H) signal at $\delta = 3.72-3.62$ ppm.

The composition of PCL-*b*-PMMA, **3**, and PMMA-*b*-PCL-*b*-PMMA, **6**, copolymers was determined by NMR using the methyl group signals at $\delta = 4.15-4.05$ ppm (CH_2O) for PCL and $\delta = 3.69-3.49$ ppm (OCH_3) for PMMA.

Tacticity of MMA was determined using the singlet for CH-(CH_3)C(OOMe) at $\delta = 1.10-1.03$ (3/6*m*H*a*, *mr*) and 0.92−0.85 (3/6mH*syn*, *rr*) and one of the doublet for CH_2C(Me)(COOMe) at $\delta = 2.12-2.04$ ppm (1H*iso*, *mmm*).

Differential scanning calorimetry (DSC) analyses were performed on a Perkin-Elmer DSC-7 apparatus under nitrogen in the temperature range −70 to 150 °C with a heating rate of 10 °C min^{-1}.

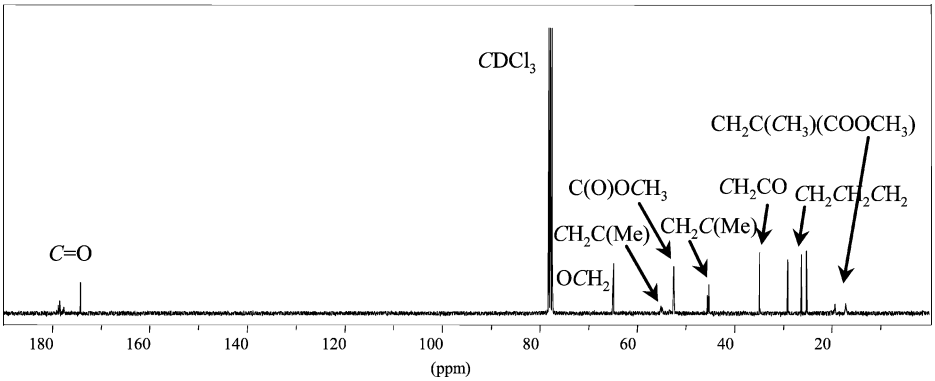

Figure 3. ^{13}C NMR spectrum in $CDCl_3$ of $PMMA_{54}$-*b*-PCL_{32}-*b*-$PMMA_{54}$, **6**.

Scheme 1. Synthesis of the Diblock PCL-*b*-PMMA, 3, Copolymer from PCL−OH, 1

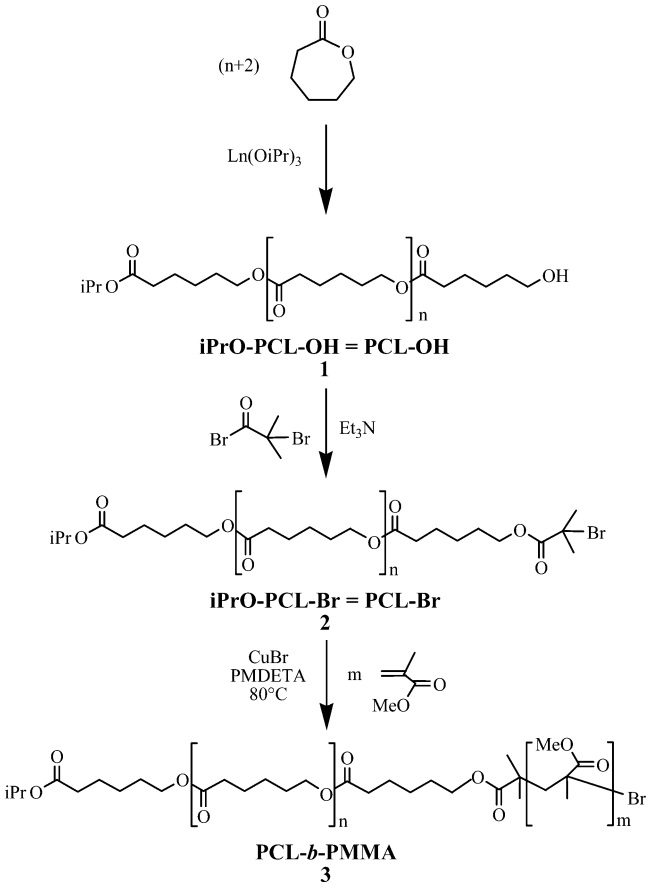

Synthesis of Bromoester End-Functionalized PCLs: *Chemical Modification of PCL−OH, **1**, to PCL−Br, **2***. Toluene (50 mL) and triethylamine (NEt_3, 421 μL, 3.02 mmol) were added to PCL−OH, **1**, ($\bar{M}_n$ = 10 700, 3.6 g, 0.34 mmol). After cooling to 0 °C, 2-bromoisobutyril bromide (223 μL, 1.8 mmol) was added and the flask was shielded from light. The temperature was then raised to room temperature, and the contents were stirred for 18 h. After filtration (removal of NEt_3Br precipitating byproduct), the filtrate was dried, dissolved in CH_2Cl_2, precipitated from MeOH, and finally dried and analyzed. The bromoester-functionalized polymer was recovered in about 90% yield after purification. ^1H NMR of **2**: δ = 5.10 (quintuplet, 1H, C*H*$(CH_3)_2$); 4.25 (t, 2H, CH_2OC(O)-CMe_2Br); 4.15 (t, $(2n + 2)$H, CH_2O); 2.39 (t, $(2n + 4)$H, C(O)-CH_2); 2.03 (s, 6H, OC(O)C(CH_3)$_2$Br); 1.71 (m, $(4n + 8)$H, CH_2CH_2CH_2); 1.48 (m, $(2n + 4)$H, $CH_2CH_2CH_2$); 1.31 (d, 6H, CH-(CH_3)$_2$) (Figure 1).

*Chemical Modification of PCL−OH_2, **4**, to PCL−Br_2, **5***. The same procedure as described for the synthesis of **2** from **1** was followed using PCL−OH_2, **4** ($\bar{M}_n$ = 12 500, 3.8 g, 0.30 mmol). The bromoester-functionalized polymer was recovered in about 90% yield after purification. ^1H NMR of **5**: δ = 5.30 (residual CH_2Cl_2); 4.18 (t, 4H, CH_2OC(O)CMe_2Br); 4.08 (t, $(2n + 2)$H, CH_2O); 2.31 (t, $(2n + 2)$H, C(O)CH_2); 1.94 (s, 12H, C(O)C(CH_3)$_2$Br); 1.67 (m, $(4n + 8)$H, CH_2CH_2CH_2); 1.40 (m, $(2n + 6)$H, $CH_2CH_2CH_2$) (Figure 2).

Typical MMA Polymerization: *Synthesis of PCL-b-PMMA Block Copolymers.* PCL−Br, **2** ($\bar{M}_n$ = 10 700, 1.5 g, 0.14 mmol), CuBr (20 mg, 0.14 mmol), and PMDETA (29 μL, 0.14 mmol) were placed in toluene (30 mL) in a flask. After cooling to 0 °C, MMA was added with a buret (4.47 mL, 42 mmol) and the reaction then maintained at 80 °C for 7 h. After removal of copper (neutral activated alumina/THF), the recovered polymer was then dried, dissolved in CH_2Cl_2, precipitated from MeOH, and finally dried and analyzed. PMMA homopolymer (negligible amount, <1%) was removed from the diblock upon dissolution of the copolymers in acetone, in which PMMA is insoluble. The diblock copolymer was isolated in about 60% yield. ^1H NMR of **3**: δ = 5.38 (residual CH_2Cl_2); 5.09 (quintuplet, 1H, C*H*$(CH_3)_2$); 4.27 (t, 2H, CH_2OC-(O)CMe_2−PMMA); 4.15 (t, $(2n + 2)$H, CH_2O); 3.69 (s, 3*m*H, OCH_3); 2.39 (t, $(2n + 4)$H, C(O)CH_2); 2.12−1.98 (m, 2*m*H*iso* + *a*, CH_2*iso* + *a*C(Me)(COOMe)); 2.03 (s, 6H, OC(O)C(CH_3)$_2$); 1.90 (s, 2*m*H*syn*, CH_2*syn*C(Me)(COOMe)); 1.71 (m, $(4n + 8)$H, CH_2CH_2CH_2); 1.48 (m, $(2n + 4)$H, $CH_2CH_2CH_2$); 1.31 (d, 6H, CH(CH_3)$_2$); 1.29 (s, 3*m*H*iso*, C(CH_3)*iso*C(OOMe)); 1.10 (s, 3*m*H*a*, C(CH_3)*a*C(OOMe)); 0.92 (s, 3*m*H*syn*, C(CH_3)*syn*C-(OOMe)) (Figure 1). ^{13}C NMR of **3** is identical to that of **6** (Figure 3).

Synthesis of PMMA-b-PCL-b-PMMA Block Copolymers. The same procedure as described for the synthesis of **3** from **2** was followed using PCL−Br_2, **5** ($\bar{M}_n$ = 12 500, 1.3 g, 0.10 mmol). PMMA homopolymer (negligible amount, <1%) was removed from the triblock upon dissolution of the copolymers in acetone, in which PMMA is insoluble. The triblock copolymer was isolated in about 77% yield. ^1H NMR of **6**: δ = 5.38 (residual CH_2Cl_2); 4.15 (t, 4H, CH_2OC(O)CMe_2−PMMA); 4.08 (t, $(2n + 2)$H, CH_2O); 3.49 (s, 6mH, OCH_3); 2.30 (t, $(2n + 2)$H, C(O)CH_2); 2.04−1.88 (m, 2*m*H*iso* + *a*, CH_2*iso* + *a*C(Me)(COOMe)); 1.95 (s, 12H, OC(O)C-(CH_3)$_2$); 1.78 (s, 2*m*H*syn*, CH_2*syn*C(Me)(COOMe)); 1.67 (m, $(4n + 8)$H, CH_2CH_2CH_2); 1.38 (m, $(2n + 6)$H, $CH_2CH_2CH_2$); 1.20 (s, unidentified); 1.17 (s, 6*m*H*iso*, C(CH_3)*iso*C(OOMe)); 1.03 (s, 6*m*H*a*, C(CH_3)*a*C(OOMe)); 0.85 (s, 6*m*H*syn*, C(CH_3)*syn*C(OOMe)) (Figure 2). ^{13}C NMR of **6**: 178.4, 178.2, 178.0, 177.1, 173.7 (PMMA−*C*(O)O, PCL−*C*(O)O); 77.2 (*C*DCl_3); 64.3 (PCL−OCH_2); 54.6 (PMMA−CH_2C(Me)(COOMe); 51.9 (PMMA−C(O)-OCH_3); 45.0, 44.7 (PMMA−CH_2*C*(Me)(COOMe)); 34.3 (PCL−*C*H_2CO); 28.5, 25.7, 24.7 (PCL−CH_2*C*H_2*C*H_2); 18.9, 16.7 (CH_2C(*C*H_3)(COOCH_3)) (Figure 3).

Preparation and Characterization of Particles. Polymeric nanoparticles from the triblock copolymers were prepared by dissolving the copolymer **6** in THF (100 mg L^{-1}, 5 mL), a good solvent for both blocks, followed by its dropwise addition (20 mL

Scheme 2. Synthesis of the Triblock PMMA-*b*-PCL-*b*-PMMA, 6, Copolymer from PCL−OH_2, 4

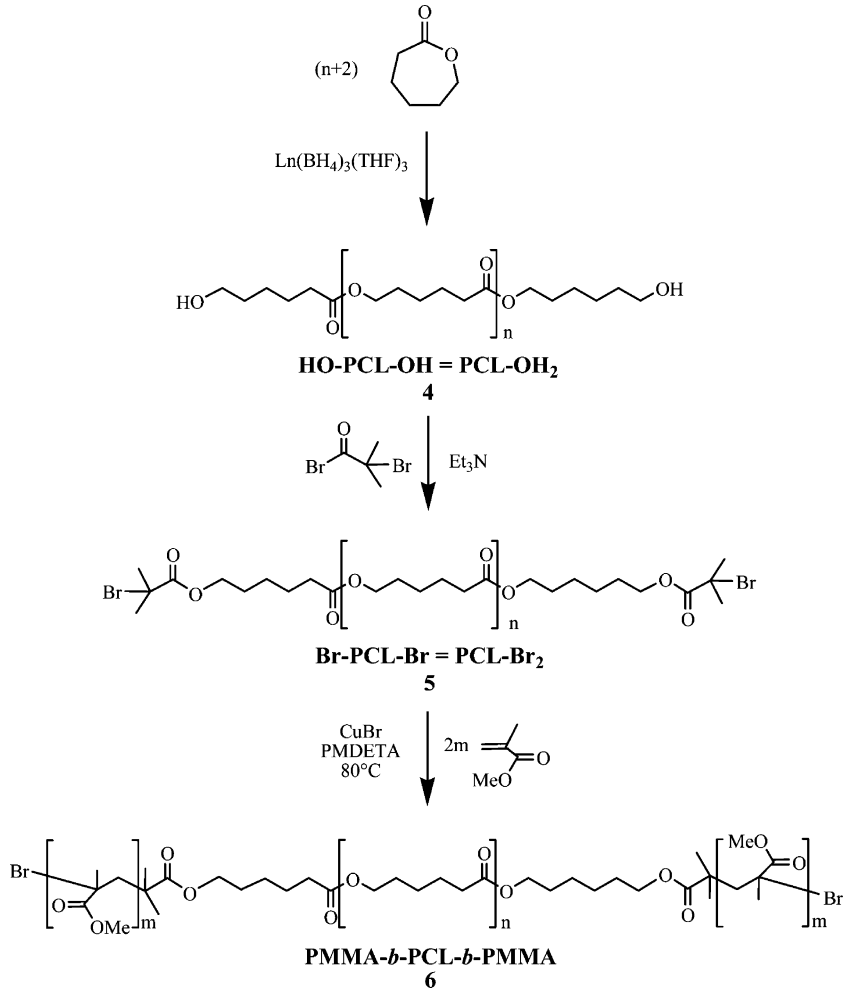

Table 1. Polymer Features of PCL−OH, 1, and PCL−Br, 2

	PCL−OH, **1**				PCL−Br, **2**				
run	$\bar{M}_{n,SEC}$[a] (g mol^{-1})	$\bar{M}_w/\bar{M}_n$[b]	$\overline{DP}n$[c]	$\bar{M}_{n,NMR}$[d] (g mol^{-1})	$\bar{M}_{n,theo}$[e] (g mol^{-1})	$\bar{M}_{n,SEC}$[a] (g mol^{-1})	$\bar{M}_w/\bar{M}_n$[b]	$\overline{DP}n$[c]	$\bar{M}_{n,NMR}$[d] (g mol^{-1})
1	3350	1.1	29	3380	3400	3300	1.2	29	3440
2	6600	1.1	58	6690	6800	7200	1.2	63	7320
3	9500	1.1	83	9540	9600	9400	1.1	83	9600
4	10 700	1.4	94	10 790	10 800	10 700	1.4	95	10 970

[a] SEC values of the precipitated polymer samples. [b] Molar mass distribution values calculated from SEC chromatogram traces. [c] Number average degree of polymerization determined from ^{1}H NMR analysis. [d] Molar mass values determined from ^{1}H NMR analysis and calculated from $\overline{DP}n \times 114 + 59$ (O^iPr) + 17 (OH)/80 (Br). [e] Theoretical molar mass values calculated from $\bar{M}_{n,SEC}$ (PCL−OH) − (17(OH) + 80(Br)).

Table 2. Polymer Features of PCL−OH_2, 4, and PCL−Br_2, 5

	PCL−OH_2, **4**				PCL−Br_2, **5**				
run	$\bar{M}_{n,SEC}$[a] (g mol^{-1})	$\bar{M}_w/\bar{M}_n$[b]	$\overline{DP}n$[c]	$\bar{M}_{n,NMR}$[d] (g mol^{-1})	$\bar{M}_{n,theo}$[e] (g mol^{-1})	$\bar{M}_{n,SEC}$[a] (g mol^{-1})	$\bar{M}_w/\bar{M}_n$[b]	$\overline{DP}n$[c]	$\bar{M}_{n,NMR}$[d] (g mol^{-1})
1	3600	1.1	32	3680	3700	3600	1.1	32	3810
4	12 500	1.4	109	12 460	12 600	12 500	1.5	109	12 590

[a] SEC values of the precipitated polymer samples. [b] Molar mass distribution values calculated from SEC chromatogram traces. [c] Number average degree of polymerization determined from ^{1}H NMR analysis. [d] Molar mass values determined from ^{1}H NMR analysis and calculated from $\overline{DP}n \times 114 + (2 \times 17$ (OH))/(2 × 80 (Br). [e] Theoretical molar mass values calculated from $\bar{M}_{n,SEC}$ (PCL−OH_2) − (2 × 17 (OH)) + (2 × 80 (Br)).

h^{-1}) to a solution of water (5 mL) at 23 °C under stirring. The residual THF was then removed by evaporation under nitrogen at ambient pressure and temperature. The resulting solution was then diluted 20 times.

The hydrodynamic diameter of the PMMA−PCL−PMMA particles was determined by dynamic light scattering (DLS) in water at a 90° angle at 20 °C on a MALVERN apparatus (Zetasizer 3000 HS) equipped with a He−Ne laser source (633 nm). Samples for imaging by atomic force microscopy (AFM) analyses were prepared by deposition of aqueous suspension of the above copolymer **6** on a mica substrate. Practically, one drop of a dilute aqueous suspension (5 mg L^{-1}) was deposited on a 1 × 1 cm^2 freshly cleaved mica substrate. Samples were analyzed after complete evaporation of the solvent at room temperature. The AFM image is shown as

Table 3. PCL-*b*-PMMA, 3, Copolymers Features

run	PCL−Br $\bar{M}_{n,SEC}$[a] (g mol^{-1})	$[PCL-Br]_0$[b] (mmol L^{-1})	$[MMA]_0$ (mmol L^{-1})	$[MMA]_0/[PCL-Br]_0$	MMA conversion[c] (%)	$\bar{M}_{n,theo}$[d] (g mol^{-1})	composition[c] PCL:PMMA (%)	$\bar{M}_{n,SEC}$[e] (g mol^{-1})	$\bar{M}_w/\bar{M}_n$[f]	$\overline{DP}n$[g] PCL−PMMA	$\bar{M}_{n,NMR}$[h] (g mol^{-1})	tacticity[c] (%) *rr*−*mr*−*mm*
1	9400	5.8	507	87	20	11 450	80:20	11 200	1.2	80−20	11 260	60−34−6
2	10 700	7.3	2320	317	55	28 100	33:67	32 000	1.2	94−195	30 360	58−36−6
3	10 700	10.0	2264	226	60	24 300	34:66	30 750	1.2	94−182	29 060	62−33−5

[a] SEC values of the precipitated polymer samples (Table 1). [b] $[PCL-Br]_0 = [Br^-]_0$. [c] Determined by ^{1}H NMR analysis. [d] Calculated from $\bar{M}_{n,SEC}$ (PCL−Br) + $[MMA]_0/[PCL-Br]_0 \times 100 \times$ Conversion (MMA). [e] Molar mass values determined from SEC using the corresponding correction coefficient and composition of each block. [f] Molar mass distribution values calculated from SEC chromatogram traces. [g] Number average degree of polymerization determined from ^{1}H NMR analysis. [h] Molar mass values determined from ^{1}H NMR and calculated from $\overline{DP}n_{PCL} \times 114 + 59$ (O^iPr) + $\overline{DP}n_{PMMA} \times 100 + 80$(Br).

Table 4. PMMA-*b*-PCL-*b*-PMMA, 6, Copolymers Features

run	PCL−Br_2 $\bar{M}_{n,SEC}$[a] (g mol^{-1})	$[PCL-Br_2]_0$[b] (mmol L^{-1})	$[MMA]_0$ (mmol L^{-1})	$[MMA]_0/[PCL-Br_2]_0$	MMA conversion[c] (%)	$\bar{M}_{n,theo}$[d] (g mol^{-1})	composition[e] PCL:PMMA (%)	$\bar{M}_{n,SEC}$[f] (g mol^{-1})	$\bar{M}_w/\bar{M}_n$[g]	$\overline{DP}n$[h] PMMA−PCL−PMMA	$\bar{M}_{n,NMR}$[i] (g mol^{-1})	tacticity[e] (%) *rr*−*mr*−*mm*
1	3600	5.5	613	111	70	11 370	23:77	25 100	1.2	54−32−54	14 610	57−35−8
2	3600	2.5	890	356	77	31 010	11:89	44 200	1.3	133−32−133	30 330	57−35−8
3	12 500	0.8	467	584	30	30 020	35:65	59 300	1.6	99−109−99	32 390	57−34−9
4	12 500	0.7	891	1273	40	63 420	17:83	96 850	1.3	258−109−258	64 190	58−34−8

[a] SEC values of the precipitated polymer samples (Table 2). [b] $2[PCL-Br_2]_0 = [Br^-]_0$. [c] Determined by gravimetry. [d] Calculated from $\bar{M}_{n,SEC}$ (PCL−Br_2) + $[MMA]_0/[PCL-Br_2]_0 \times 100 \times$ conversion (MMA). [e] Determined from ^{1}H NMR analysis. [f] Molar mass values determined from SEC using the corresponding correction coefficient and composition of each block. [g] Molar mass distribution values calculated from SEC chromatogram traces. [h] Number average degree of polymerization determined from ^{1}H NMR analysis. [i] Molar mass values determined from ^{1}H NMR and calculated from $\overline{DP}n_{PCL} \times 114 + \overline{DP}n_{PMMA} \times 100 + (2 \times 80$ (Br))

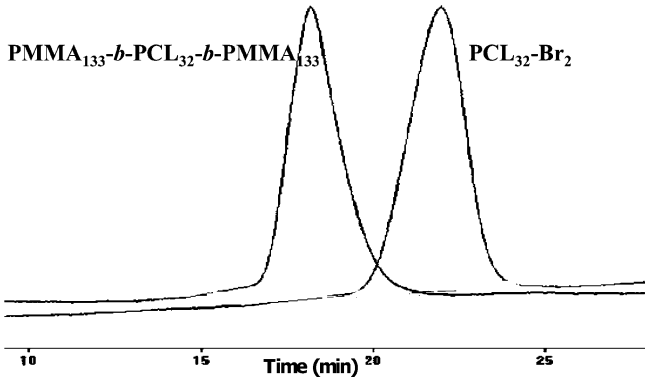

Figure 4. SEC traces of $PCL_{32}-Br_2$, **5**, and the corresponding triblock $PMMA_{133}$-*b*-PCL_{32}-*b*-$PMMA_{133}$, **6**.

recorded. Polarized optical microscopy images were (otherwise) obtained using a Leitz optical microscope equipped with a camera (SONY) in combination with a Mettler-Toledo FP2 hot stage. The films were obtained after cooling from the melt at 10 K min^{-1} on a glass plate.

Results and Discussion

A. Chemical Modification of Hydroxyl-Functionalized PCLs PCL−OH, 1, and PCL−OH_2, 4, to Their Respecitve Bromo Analogues PCL−Br, 2, and PCL−Br_2, 5. Monohydroxyl- and dihydroxyl-functionalized PCLs, PCL-OH, **1**, and PCL-OH_2, **4**, were synthesized by ring-opening polymerization (ROP) using La(O^iPr)$_3$ and Sm(BH_4)$_3$(THF)$_3$ as initiators, respectively, according to previously described procedures (Schemes 1 and2).[16−18] These well-established processes allow a quantitative and controlled polymerization of CL within specific conditions thereby offering, within less than 15 min in THF at 21 °C, well-defined mono- and dihydroxy polymers (Tables 1 and 2). NMR characterization of **1** and **4** depicted, in particular, the typical CH_2OH signals at $\delta = 3.72-3.62$ ppm (^{1}H) and $\delta = 32.4$ ppm (^{13}C) confirming the hydroxyl-terminated PCL structures (Figures 1 and 2).

These hydroxyl macroligands (**1, 4)** were then chemically modified to the corresponding bromo analogue PCLs, PCL−Br, **2**, and PCL−Br_2, **5**, respectively, in order to be used as

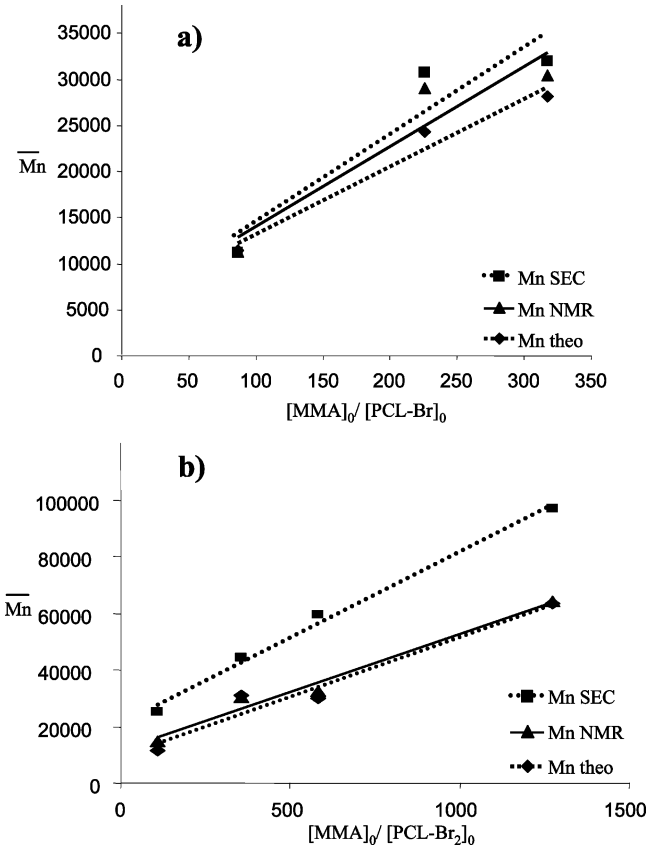

Figure 5. $\bar{M}_n$ vs $[MMA]_0/[PCL-Br_{1/2}]_0$ for (a) PCL-*b*-PMMA and (b) PMMA-*b*-PCL-*b*-PMMA (Tables 3 and 4).

macroinitiators for the preparation of the acrylate block via atom transfer radical polymerization (ATRP) (Schemes 1 and 2). Quantitative esterification of the hydroxyl end group(s) to the bromoester function(s) was performed using 2-bromoisobutyryl bromide in presence of NEt_3. The polymer molar mass and molar mass distribution stayed constant after chemical treatment showing that the main PCL chain remains unaltered (Tables 1 and 2). ^{1}H NMR analyses confirm the presence of the ester end group(s) through the disappearance of the original −CH_2OH

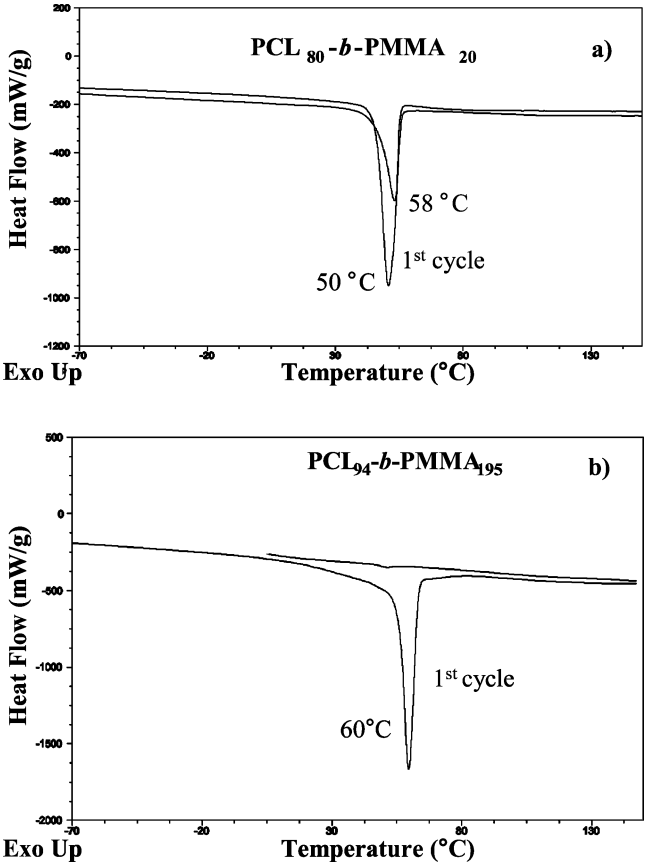

Figure 6. DSC plots of diblock copolymers: (a) PCL_{80}-*b*-$PMMA_{20}$ and (b) PCL_{94}-*b*-$PMMA_{195}$.

triplet signal of **1** and **4** ($\delta = 3.72-3.62$ ppm) along with the appearance in both **2** and **5** of the methyl groups of the bromoester $-OC(O)C(CH_3)_2Br$ at $\delta = 2.03-1.94$ ppm and of the methylene proton $-CH_2OC(O)C(Me)_2Br$ at $\delta = 4.25-4.18$ ppm, other peaks being assigned to the protons of the PCL chain (Figures 1 and 2). This procedure is a simplified adaptation of the one described by Chen for making PCL−Br and of that by Fraser for the preparation of bipyridine (bipy)-linked $(PCL-Br)_2$ from the bis(monohydroxyl PCL) macroligand HO−PCL−bipy−PCL−OH.[21,22] The present results demonstrate that both PCL hydroxyl end groups of the α,ω-dihydroxy-functionalized PCL have been simultaneously and successfully transformed into the bromo analogues. In addition, the alkoxy end group of *i*PrO−PCL−OH, **1**, remains unaffected during the OH/Br modification, as shown by the appropriate integration of the signals of $-C(O)OCH(CH_3)_2$ at $\delta = 5.10$ and 1.31 ppm (Figures 1 and 2). These bromo-functionalized PCL macroinitiators $PCL-Br_{1/2}$, **2**−**5**, then afforded a smooth access to the polyester−polyacrylate block copolymers.

B. Polymerization of MMA from PCL−$Br_{1/2}$ Macroinitiators: *Synthesis and Characterization of PCL-b-PMMA and PMMA-b-PCL-b-PMMA Copolymers*. The reported syntheses of PCL/PMMA block copolymers can be gathered into three general routes. First, the block copolymerization of MMA with CL has been described via coordination−insertion polymerizations using an aluminoxane or an alkyl samarium initiator or via enzymatic routes.[23−26] The second approach involving two mechanistically distinct polymerization techniques, namely, ROP and ATRP, requires a dual/heterofunctional initiator bearing two distinct reaction sites; usually a hydroxyl group for the polymerization of the cyclic ester monomer and either a bromide or a nitroxide for that of the acrylate.[27−31] In this latter procedure,

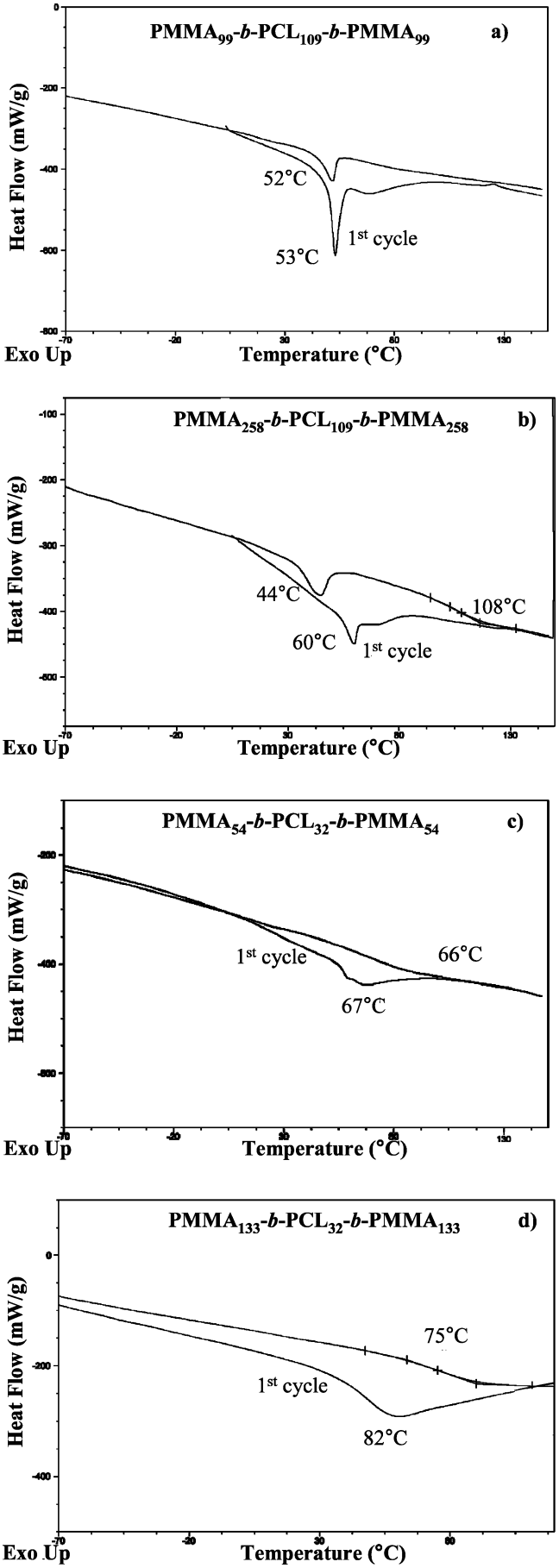

Figure 7. DSC plots of triblock copolymers: (a) $PMMA_{99}$-*b*-PCL_{109}-*b*-$PMMA_{99}$, (b) $PMMA_{258}$-*b*-PCL_{109}-*b*-$PMMA_{258}$, (c) $PMMA_{54}$-*b*-PCL_{32}-*b*-$PMMA_{54}$, and (d) $PMMA_{133}$-*b*-PCL_{32}-*b*-PMM_{133}, **6**.

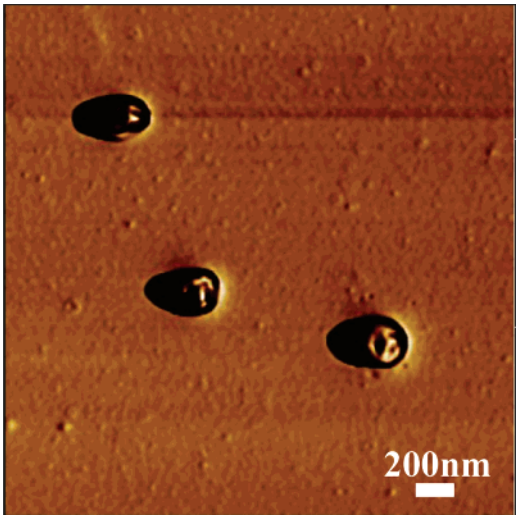

Figure 8. AFM phase image of a deposit on a mica substrate of an aqueous suspension obtained by nanoprecipitation of the triblock copolymer $PMMA_{99}$-*b*-PCL_{109}-*b*-$PMMA_{99}$, **6**.

both ROP and ATRP are always performed stepwise except in the case of the established direct one-step pathway from 2,2,2-tribromoethanol using $Al(O^iPr)_3$ and $[NiBr_2(PPh_3)_2]$.[27] Finally, the chemical modification reaction(s) of the, eventually active or isolated, first synthesized polymer block into a macroinitiator for the second monomer polymerization represents (represent) the last strategy. Usually in these latter cases, the PCL block is made first and it is either chemically[22,32−36] or photochemically[37,38] transformed. All these literature reports describe the synthesis of diblock PCL-*b*-PMMA or PMMA-*g*-PCL. However, no PCL−PMMA analogous di- and triblock copolymer sets may be synthesized from any of these procedures.

MMA was polymerized by ATRP from the *tert*-bromoester-functionalized PCL−$Br_{1/2}$, **2**, **5**. The reaction was carried out at 80 °C in toluene for 7 h in the presence of Cu(I) and the multidentate ligand pentamethyldiethylenetriamine (PMDETA) used as a catalyst.[39] The resulting copolymers *i*PrO−PCL-*b*-PMMA−Br = PCL-*b*-PMMA, **3**, and Br−PMMA-*b*-PCL-*b*-PMMA−Br = PMMA-*b*-PCL-*b*-PMMA, **6**, were isolated after precipitation in methanol (Schemes 1 and 2). Diblock and triblock copolymers of various compositions in each segment were synthesized by varying the ratio of the MMA to the bromo−PCL initiator **3** or **5** (Tables 3 and 4). The composition of the diblock PCL-*b*-PMMA, **3**, copolymers varies from lactone rich to acrylate rich type (Table 3), whereas the composition of the triblock PMMA-*b*-PCL-*b*-PMMA, **6**, remains richer (at least twice as much) in acrylate segments (Table 4). Typical ^1H and ^{13}C NMR spectra of PCLs−OH **1** and **4** and PCLs−Br **2** and **5** with the corresponding assignments are shown in Figures 1−3. NMR spectra of the copolymers **3** and **6** show the disappearance of the characteristic original $-CMe_2Br$ signal (^1H ($-CMe_2Br$) $\delta = 2.03-1.94$ ppm) thereby highlighting that the end function(s) of both polymers **2** and **5** has (have) efficiently polymerized MMA. While some PCL-*b*-PMMA copolymers have already been reported, the triblock copolymer PMMA-*b*-PCL-*b*-PMMA, **6**, represents, along with PMMA-*b*-PCL−bipyridine−PCL-*b*-PMMA,[22] the only copolymer associating two PMMA to a central polyester segment. The significant advantage of our procedure is that it affords both di- and triblock analogous copolymers, such a unique couple of copolymers being highly desirable and valuable, for instance, as biomaterials.

Size exclusion chromatography (SEC) elution curves of the copolymers, illustrated for the triblock **6** in Figure 4, show the shift to higher molar mass region after the ATRP and thus confirm efficient initiation by the bromo−PCLs **2** and **5**. The symmetric peak and the narrow molar mass distribution of the copolymers both support the absence of residual homopolymers in the final products. In addition, no homo PCL was obtained during the extraction process highlighting that the ATRP did not affect the polyester chain. Molar mass data obtained from SEC for all PCL−PMMA copolymers were measured versus polystyrene standards. While the molar masses obtained from SEC analysis for the diblock copolymers ($\bar{M}_{n,SEC}$ **3** = 11200) are in good agreement with the ones calculated ($\bar{M}_{n,theo}$ **3** = 11450, Table 3), those obtained for the triblock copolymers ($\bar{M}_{n,SEC}$ **6** = 25 100) are always significantly higher than the expected values ($\bar{M}_{n,theo}$ **6** = 11 370, Table 4). This $\bar{M}_{n,SEC}/\bar{M}_{n,theo}$ divergence arises from the difference in the hydrodynamic volumes of the triblock copolymers and of poly(styrene) standards of the same molar mass and also from the different hydrodynamic volumes between di- and triblock copolymers. Such larger $\bar{M}_{n,SEC}$ values have been observed in other polyacrylate copolymers.[40,41]

The real molar mass of PCL−PMMA block copolymers was determined by ^1H NMR analysis. The molar mass of the first block PCL−$Br_{1/2}$, **2** or **5**, was measured by SEC ($\bar{M}_{n,SEC}$ **2** = 9400, $\bar{M}_w/\bar{M}_n$ **2** = 1.1; $\bar{M}_{n,SEC}$ **5** = 3600, $\bar{M}_w/\bar{M}_n$ **5** = 1.1) and was found to be in agreement with the molar mass determined by NMR ($\bar{M}_{n,NMR}$ **2** = 9600; $\bar{M}_{n,NMR}$ **5** = 3810). The second block was polymerized and the resultant copolymer **3** or **6** was isolated and similarly analyzed by SEC ($\bar{M}_{n,SEC}$ **3** = 11 200, $\bar{M}_w/\bar{M}_n$ **3** = 1.2; $\bar{M}_{n,SEC}$ **6** = 25 100, $\bar{M}_w/\bar{M}_n$ **6** = 1.2) and NMR ($\bar{M}_{n,NMR}$ **3** = 11 260; $\bar{M}_{n,NMR}$ **6** = 14 610). Calculation of the theoretical molar mass from the ratio of monomer to initiator initial concentrations and MMA conversion gives values ($\bar{M}_{n,theo}$ **3** = 11 450; $M_{n,theo}$ **6** = 11 370) that are in close agreement with those determined by NMR for both the di- and triblock copolymers. However, the molar mass values obtained from SEC are, in the case of triblocks, nearly twice the actual values, supporting that the SEC protocol overestimates the true molar mass of the PMMA-*b*-PCL-*b*-PMMA copolymers by a factor of 2. This is not the case for the diblock copolymers, with the proportion of PMMA relative to the whole copolymer being much lower than that in the triblock. Also, for both diblock and triblock synthesis, $\bar{M}_n$ ($\bar{M}_{n,NMR}$, $\bar{M}_{n,SEC}$) increased linearly in proportion to the $[MMA]_0/[PCL-Br_{1/2}]_0$ while the narrow molar mass distribution remained constant ($\bar{M}_w/\bar{M}_n$ average value for **3** = 1.2 and for **6** = 1.35) over the whole range of catalytic concentrations (Figure 5). This verifies that the growth of the second block by ATRP is consistent with that observed in a controlled and "living" process.

Differential scanning calorimetry (DSC) curves of the copolymers of various compositions (PMMA:PCL) are presented in Figures 6 and 7. The thermograms (first heating cycle) of the diblock copolymers **3**, PCL_{80}-*b*-$PMMA_{20}$ (0.25:1) and PCL_{94}-*b*-$PMMA_{195}$ (2.1:1) alternatively rich in PCL and PMMA, respectively (with similar tacticity), exhibit a melting temperature specific to the PCL block (T_m = 50 °C, ΔH = 27.7 J g^{-1} (top trace) and T_m = 60 °C, ΔH = 44.25 J g^{-1} (bottom trace) of Figure 6). No glass transition temperature is observed for PCL at −60 °C or for PMMA at 110−130 °C. During the second heating cycle the T_m of PCL could only be detected at 58 °C (bottom trace) for the copolymer having the greatest polyester content, PCL_{80}-*b*-$PMMA_{20}$. This latter T_m is 8 °C higher than that of the first run with a weaker melting enthalpy most likely because the PCL crystalline structures, which have been destroyed during the first melting run, do not grow back

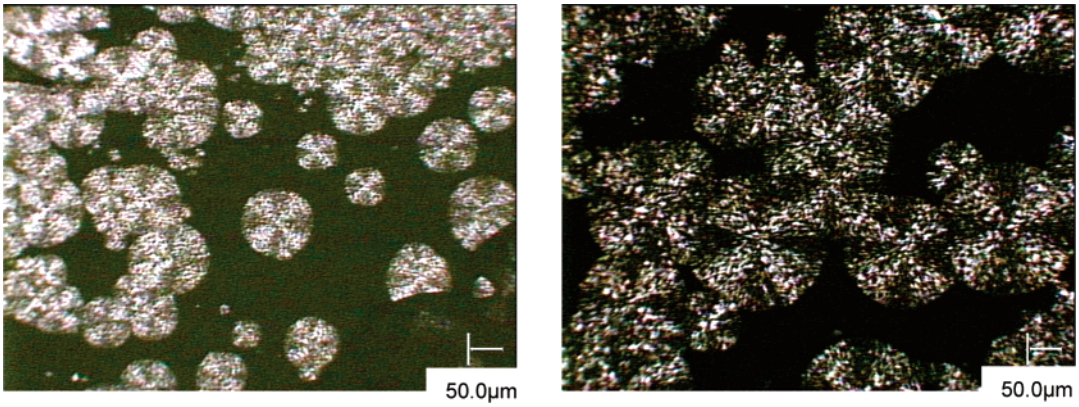

Figure 9. Optical micrograph images taken under crossed polarizers of a film obtained after heating the triblock copolymer $PMMA_{99}$-PCL_{109}-$PMMA_{99}$, **6**.

to the same extent during the short heating time of the second run. This also suggests that the greater the amount of PMMA the more difficult it is for the PCL to self-organize upon cooling down.

DSC curves of the triblock copolymers of various compositions are gathered in Figure 7. The copolymer having the smallest amount of PMMA relative to the PCL block (1.8:1), $PMMA_{99}$-*b*-PCL_{109}-*b*-$PMMA_{99}$, only displays, on both heating cycles, a melting endotherm at 52−53 °C specific to the PCL segment; this transition appears at a temperature lower than that observed for PCL homopolymers, highlighting that the crystallization process of PCL is disturbed most likely as a result of the incorporation of PMMA into the copolymers (Figure 7a). These thermograms differ from those of the diblock copolymers with segments of similar relative size, PCL_{94}-*b*-$PMMA_{195}$ (2.1:1). This thus highlights significant structural differences between a diblock and a triblock architecture, which clearly do not behave similarly. When the the PCL block is kept constant, an increase in the PMMA content (4.7:1) still allows the melting temperature of the PCL block to be observed; in $PMMA_{258}$-*b*-PCL_{109}-*b*-$PMMA_{258}$, the PCL exhibits a T_m at 60 °C in the first heating cycle (ΔH = 1.2 J g^{-1}, bottom trace) and at 44.25 °C in the second cycle (top trace, Figure 7b). Similar to what was noticed with the diblock copolymers (Figure 7a,b), increasing the amount of PMMA prevents the crystalline structures of the PCL block, which have been destroyed during the first melting run, to grow back to the same extent during the short heating time of the second run. The ΔH melting enthalpy is lower for the PCL-smaller copolymer (1.2 J g^{-1} for $PMMA_{258}$-*b*-PCL_{109}-*b*-$PMMA_{258}$; 5.3 J g^{-1} for $PMMA_{99}$-*b*-PCL_{109}-*b*-$PMMA_{99}$, Figure 7). In addition, increasing the length of each PMMA block on going from $PMMA_{99}$-*b*-PCL_{109}-*b*-$PMMA_{99}$ to $PMMA_{258}$-*b*-PCL_{109}-*b*-$PMMA_{258}$ allows the glass transition of PMMA to be observed during the second heating cycle at 108 °C (Figure 7b).

The copolymers having the smallest PCL block length (-PCL_{32}-), $PMMA_{54}$-*b*-PCL_{32}-*b*-$PMMA_{54}$ (3.4:1) and $PMMA_{133}$-*b*-PCL_{32}-*b*-$PMMA_{133}$ (8.3:1), display a weak and broad transition for the T_m of the PCL block (67 and 82 °C, respectively, Figure 7c,d). In these two copolymers, no melting endotherm is observed for the PCL block on the second heating cycle; only a slight inflection of the slope is recorded (66 and 75 °C) at a temperature that is higher for the copolymer with the largest content of PMMA, $PMMA_{133}$-*b*-PCL_{32}-*b*-$PMMA_{133}$. This underlines again the influence of the PMMA block on the PCL organization, which moves less freely in the presence of larger amount of PMMA and thus is not as crystalline as in the case with less PMMA around. Although the triblock copolymer $PMMA_{133}$-*b*-PCL_{32}-*b*-$PMMA_{133}$ has the greatest amount of PMMA relative to PCL (8.3:1), the PMMA glass transition temperature could not be observed, similar to what was noted with the other PCL-short triblock copolymer $PMMA_{54}$-*b*-PCL_{32}-*b*-$PMMA_{54}$ (3.4:1) (Figure 7c,d).

All these thermal analyses results strongly suggest that both the ratio of PMMA to PCL and the length of each block in combination with the intrinsic crystallinity of each polymer type plays a determinant role on the overall behavior of the copolymers.

C. Polymer Particles of PMMA-*b*-PCL-*b*-PMMA. To determine the influence (especially of the crystallinity) of both type of blocks forming a copolymer on the overall organization of the copolymer is important in order to adjust the final properties of the particles formed in the context of drug-delivery applications.[4,5] Nanoprecipitation is a general method that allows the preparation of nanoparticles in aqueous medium from hydrophobic systems such as PCL or poly(L-lactide-*co*-glycolide).[42−45] This requires two miscible solvents, one being a good solvent of the copolymer and the other a nonsolvent. Particles of the triblock copolymer **6** were thus obtained using THF as the solvent and water as the nonsolvent. The copolymer solution was added dropwise to H_2O, and the particles formed almost immediately along with the formation of a milky suspension. Upon getting in contact with water, the solvent drops divide themselves into smaller entities into which water then diffuses more easily, ultimately leading to aggregation of the polymeric chains and therefore to their precipitation.[43,44]

The solution self-assembling behavior of the PMMA-*b*-PCL-*b*-PMMA copolymers was investigated by measuring the hydrodynamic diameter by dynamic light scattering (DLS).

The triblock copolymers display particle sizes in the range 250−300 nm. The sizes of the nanospheres increase with the relative amount of CL in the triblock copolymer. Formation of such large objects most likely results from the reduced solvation ability of the shorter PMMA segments, which thereby cannot aggregate into closer packed particles.

Deposits on a mica substrate of an aqueous suspension obtained by nanoprecipitation of the triblock copolymer **6** were analyzed by atomic force microscopy (AFM) (Figure 8). All four triblock copolymers synthesized (Table 4) were similarly investigated. The images obtained from all triblock copolymers **6** show a quite spherical morphology composed of particles 190−280 nm, exhibiting a PMMA inner core surrounded by outer PCL corona as illustrated in Figure 8 with the copolymer $PMMA_{99}$-*b*-PCL_{109}-*b*-$PMMA_{99}$ (the soft PCL segments appear darker than the stiff and brighter PMMA blocks). The morphology of the same copolymer $PMMA_{99}$-PCL_{109}-$PMMA_{99}$ was also

investigated by optical microscopy (Figure 9). The micrograph exhibits a typical Maltese cross due to a spherulitic structure. This supported the crystalline nature of the triblock copolymers as observed by DSC.

Conclusion

Novel PMMA−PCL multiblock copolymers were synthesized by using bromopolyesters, initially synthesized by ROP of PCL, as macroinitiators for the ATRP of MMA. Combination of these two well-controlled processes affords well-defined copolymers of a wide array of composition, ranging from polyester rich to polyacrylate rich as well as from diblock to triblock copolymers (especially) PCL-*b*-PMMA, **3**, and PMMA-*b*-PCL-*b*-PMMA, **6**. Both the PMMA:PCL ratio and the size of each constituting block significantly influence the properties of the copolymers as highlighted especially by thermal analyses. These copolymers represent a unique set of PCL/PMMA analogous di- and triblock copolymers, of which the triblock self-assembling behavior has been studied in detail for the first time. Self-assembling of triblock copolymers **6** leads to the formation of particles, and the size of the particles as determined by DLS (250−300 nm) increases with respect to the PCL content. The morphology of these same triblock copolymers examined by AFM showed quite spherical particles of diameter ranging from 190 to 280 nm and spherulitic structures, which was further confirmed by optical microscopic analyses. Substitution of the MMA block(s) by (a) potentially hydrophilic acrylate unit(s) as well as tuning the properties (crystallinity, biodegradability, etc.) of the hydrophobic polyester moiety by varying its nature will allow for further investigations on the self-assembling behavior of such amphiphilic systems into nanoparticles. Biomaterials derived from these copolymers will find applications as drug-delivery vehicles or in tissue repair.[11−14]

Acknowledgment. We thank Emanuel Ibarboure for useful discussions and help in recording the DSC data and Dr. Michel Schappacher for acquiring the AFM images and for valuable information.

References and Notes

(1) Noshay, N.; McGrath, J. E. *Block Copolymers*; Academic press: London, U.K., 1997.
(2) Hamley, I. W. *The Physics of Block Copolymers*; Oxford Science Publications: Oxford, U.K., 1998.
(3) Alexandridis, P. *Curr. Opin. Colloid Interface Sci.* **1996**, *1*, 490−501.
(4) Allen, C.; Maysinger, D.; Eisenberg, A. *Colloids Surf., B: Biointerfaces* **1999**, *16*, 3−27.
(5) Adams, M. L.; Lavasanifar, A.; Kwon, G. S. *J. Pharm. Sci.* **2003**, *92*, 1343−1355.
(6) Nishiyama, N.; Kataoka, K. *Adv. Polym. Sci.* **2006**, *193*, 67−101.
(7) Albertsson, A.-C.; Varma, I. K. *Biomacromolecules* **2003**, *4*, 1466−1486.
(8) Schappacher, M.; Soum A.; Guillaume, S. M. *Biomacromolecules* **2006**, *7*, 1373−1379.
(9) Le Hellaye, M.; Schappacher, M.; Soum, A.; Guillaume, S. M. Macro 2006, Proceedings of the 41st International Symposium on Macromolecules: Wiley-VCH: Weinheim, 2006.
(10) Le Hellaye, M.; Schappacher, M.; Soum, A.; Guillaume, S. M. Unpublished work.
(11) Abraham, G. A.; Gallardo, A.; San Roman, J.; Fernandez-Mayoralas, A.; Zurita, M.; Vaquero, J. *J. Biomater. Res. A* **2003**, *64*, 638−647.
(12) Li, Y.-Y.; Zhang, X.-Z.; Cheng, H.; Zhu, J.-L.; Cheng, S.-X.; Zhuo, R.-X. *Macromol. Rapid Commun.* **2006**, *27*, 1913−1919.
(13) Hong, S. W.; Kim, K. H.; Huh, J.; Ahn, C.-H.; Jo, W. H. *Macromol. Res.* **2005**, *13*, 397−402.
(14) Shanmugananda, M. K.; Zhang, Q.; Remsen, E. E.; Wooley, K. L. *Polym. Mater. Sci. Eng.* **2001**, *84*, 1073−1074.
(15) Palard, I.; Schappacher, M.; Soum, A.; Guillaume, S. M. *Polym. Int.* **2006**, *55*, 1132−1137.
(16) Guillaume, S. M.; Schappacher, M.; Soum, A. *Macromolecules* **2003**, *36*, 54−60.
(17) Palard, I.; Soum, A.; Guillaume, S. M. *Macromolecules* **2005**, *38*, 6888−6894.
(18) Palard, I.; Soum, A.; Guillaume, S. M. *Chem. Eur.*−*J.* **2004**, *10*, 4054−4062.
(19) Barros, N.; Schappacher, M.; Dessuge, P.; Maron, L; Guillaume, S. M. *Chem.*−*Eur. J.* **2007**, in press.
(20) Kricheldorf, H. R.; Rost, S. *Macromolecules* **2005**, *38*, 8220−8226.
(21) Chen, Y. M.; Wulff, G. *Macromol. Rapid Commun.* **2002**, *23*, 59−63.
(22) Johnson, R. M.; Fraser, C. L. *Macromolecules* **2004**, *37*, 2718−2727.
(23) Wu, B.; Lenz, R. W.; Hazer, B. *Macromolecules* **1999**, *32*, 6856−6859.
(24) Yamashita, M.; Takemoto, Y.; Yasuda, H. *Macromolecules* **1996**, *29*, 1798−1806.
(25) Zhou., J.; Villarroya, S.; Wang, W.; Wyatt, M. F.; Duxbury, C. J.; Thurecht, K. J.; Howdle S. M. *Macromolecules* **2006**, *39*, 5352−5358.
(26) De Geus, M.; Schormans, L.; Palmans, A. R. A.; Konig, C. E.; Heise, A. *J. Polym. Sci., Part A: Polym. Chem.* **2006**, *44*, 4290−4297.
(27) Mecerreyes, D.; Moineau, G.; Dubois, P.; Jérôme, R.; Hedrick, J. L.; Hawker, C. J.; Malmström, E. E.; Trollas, M. *Angew. Chem., Int. Ed.* **1998**, *37*, 1274−1276.
(28) Hawker, C. J.; Hedrick, J. L.; Malmström, E. E.; Trollas, M.; Mecerreyes, D.; Moineau, G.; Dubois, P.; Jérôme, R. *Macromolecules* **1998**, *31*, 213−219.
(29) Wang, W.; Yin, Z.; Detrembleur, C.; Lecomte, P.; Lou, X.; Jérôme, R. *Macromol. Chem. Phys.* **2002**, *203*, 968−974.
(30) Mecerreyes, D.; Trollas, M.; Hedrick, J. L. *Macromolecules* **1999**, *32*, 8753−8759.
(31) Meyer, A.; Palmans, R. A.; Loontjens, T.; Heise, A. *Macromolecules* **2002**, *35*, 2873−2875.
(32) Mespouille, L.; Degée, Ph.; Dubois, Ph. *Eur. Polym. J.* **2005**, *41*, 1187−1195.
(33) Eroglu, M. S.; Hazer, B.; Baysal, B. M. *J. Appl. Polym. Sci.* **1998**, *68*, 1149−1157.
(34) Motala-Timol, S.; Bhaw-Luximon, A.; Jhurry, D. *Macromol. Symp.* **2006**, *231*, 69−80.
(35) Ydens, I.; Degée, P.; Dubois, P.; Libiszowski, J.; Duda, A.; Penczek, S. *Macromol. Chem. Phys.* **2003**, *204*, 171−179.
(36) Mecerreyes, D.; Atthoff, B.; Boduch, K. A.; Trollas, M.; Hedrick, J. L. *Macromolecules* **1999**, *32*, 5175−5182.
(37) Degirmenci, M.; Hizal, G.; Yagci, Y. *Macromolecules* **2002**, *35*, 8265−8270.
(38) Hedrick, J. L.; Trollas, M.; Hawker, C. J.; Atthoff, B.; Claesson, H.; Heise, A.; Miller, R. D.; Mecerreyes, D.; Jérôme, R.; Dubois, Ph. *Macromolecules* **1998**, *31*, 8691−8705.
(39) Matyjaszewki, K.; Nakagawa, Y.; Jasieczek, C. B. *Macromolecules* **1998**, *31*,1535−1541.
(40) Beers, K. L.; Boo, S.; Gaynor, S. G.; Matyjaszewski, K. *Macromolecules* **1999**, *32*, 5772−5776.
(41) Yuan, W.; Yuan, J.; Zhou, M.; Sui, X. *J. Polym. Sci.* **2006**, *44*, 6575−6586.
(42) Fessi, H.; Devissaguet, J.-P.; Puisieux, F.; Thies, C. C.N.R.S., *FR* 2,-608,988, 1988.
(43) Niwa, T.; Takeuchi, H.; Hino, T.; Kunou, N.; Kawashima, Y. *J. Controlled Release* **1993**, *25*, 89−98.
(44) Molpeceres, J.; Guzman, M.; Aberturas, M. R.; Chacon, M.; Berges, L. *J. Pharm. Sci.* **1996**, *85*, 206−213.
(45) Ge, H.; Hu, Y.; Song, J.; Ren, T. *J. Appl. Polym. Sci.* **2000**, *75*, 874−882.

MA070417Q